

Automatic Test Bench for Selected Transmission Parameters of Power Line Conductors

Łukasz Chruszczyk

Abstract—This paper presents automatic test bench used for measurement of selected high frequency parameters of a power copper line. The aim is fast estimation of line behavior in context of Power Line Communication (PLC). The hardware interface uses sinusoidal waveform generator, digital oscilloscope and a PC-class computer. The software interface created in LabVIEW environment performs signal processing and data presentation.

Keywords—LabVIEW, power line measurements, Power Line Communication, amplitude spectrum, phase spectrum, crosstalk measurement

I. INTRODUCTION

THE submitted manuscript presents automatic stand for measurements of selected high frequency parameters of a standard voltage (230 VAC, 50 Hz) power line. Fast estimation of a line high frequency parameters is helpful in determining PLC communication limits and if such transmission can be successful at all [1–6]. The greatest challenges in PLC transmission are related with their uncertainty and time variation [7–13].

Generally the line under test can be any copper paired conductor, however the article focuses on a PLC context. Therefore the measurement frequencies have been limited to range 10 kHz – 10 MHz.

The hardware part of the stand uses PC-class computer, Rigol DG1032z arbitrary waveform generator and Tektronix DPO3012 oscilloscope. Particular devices can be connected by USB or Ethernet bus. The hardware control and data readout are performed by means of SCPI commands through LabVIEW environment and VISA/IVI drivers [14]. The last can be already included or downloaded from *National Instruments* or device manufacturer's web site. More expensive or popular equipment is directly supported by LabVIEW in form of ready-to-use blocks. Elsewhere, SCPI commands (e.g. *DG1000 Programming Guide*) must be used directly.

The software part, written in LabVIEW, controls the devices, performs signal processing and data presentation. Front panel of the virtual instrument (VI) is presented on fig. 1. The VI allows selection of generator output voltage level, oscilloscope initial gain, initial and final test frequencies, sweep type (linear or logarithmic) and number of frequency points. During measurement, the results are presented to the user in real-time and amplitude/phase characteristics is drawn. Simplified algorithm is presented in the fig. 2. The program loop iterates as many times as selected number of frequency points.

Ł. Chruszczyk is with Silesian University of Technology; Faculty of Automatic Control, Electronics and Computer Science; Gliwice, Poland (e-mail: lch@polsl.pl).

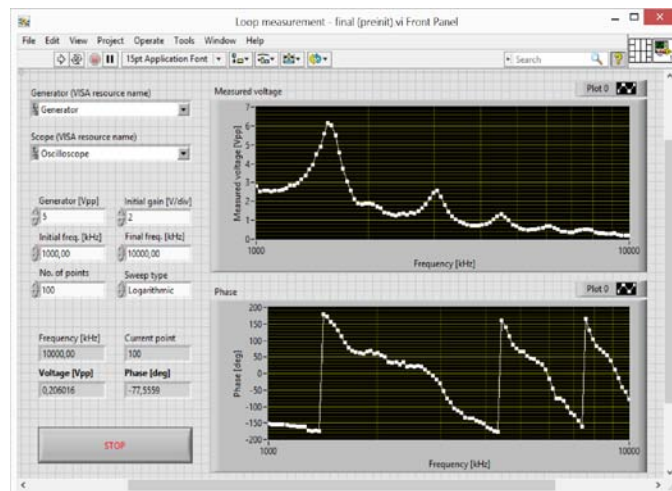


Fig. 1. Front panel of the LabVIEW virtual instrument (VI)

The initial oscilloscope gain should be set by the user, because the *auto-setup* feature has not been used. First reason is quite frequent failure of this function, especially for low frequency or noisy signals. The other reason is long *auto-setup* time: ca. 3 s. Instead, the oscilloscope current gain (scale S_i) is set manually based on the previous peak-to-peak measurement M_{i-1} (eq. 1). The result is amplitude of measured signal near half of the scope screen. The constant 4 results from total 8 horizontal divisions. This is a compromise between accurate measurement and risk of out-of-screen amplitude escape.

$$S_i [V] = \frac{M_{i-1} [V_{pp}]}{4} \quad (1)$$

The oscilloscope performs measurements itself: peak-to-peak voltage on channels 1 and 2. There is no need to send whole waveform to the PC and analyse it in software, which shortens processing time. Selection of peak-to-peak measurement function is preferred over other possibilities. E.g. amplitude measurement requires additional measurement of a waveform mean value; cyclic RMS measurement requires additional measurement of a waveform period. Elimination of additional readouts reduces final measurement uncertainty. Because levels of the measured signals are relatively high (at least hundreds of mVpp) and with negligible noise, no averaging has been utilized.

Similar procedure is used to set the oscilloscope time base T_i . Because generated (and received) signal frequency f_i is known, there is no need to measure it by the scope – thus again one source of uncertainty is eliminated (eq. 2). The result are at

least 2 periods of the measured signal fit on the scope screen. The constant 6000 results from total 12 vertical divisions.

$$T_i [s] = \frac{f_i [kHz]}{6000} \quad (2)$$

Such *manual auto-setup* works more stable (for small frequency steps) and much faster: below 1 s per measurement.

After all measurements are complete, the results are saved to CSV-type text file (Excel compatible).

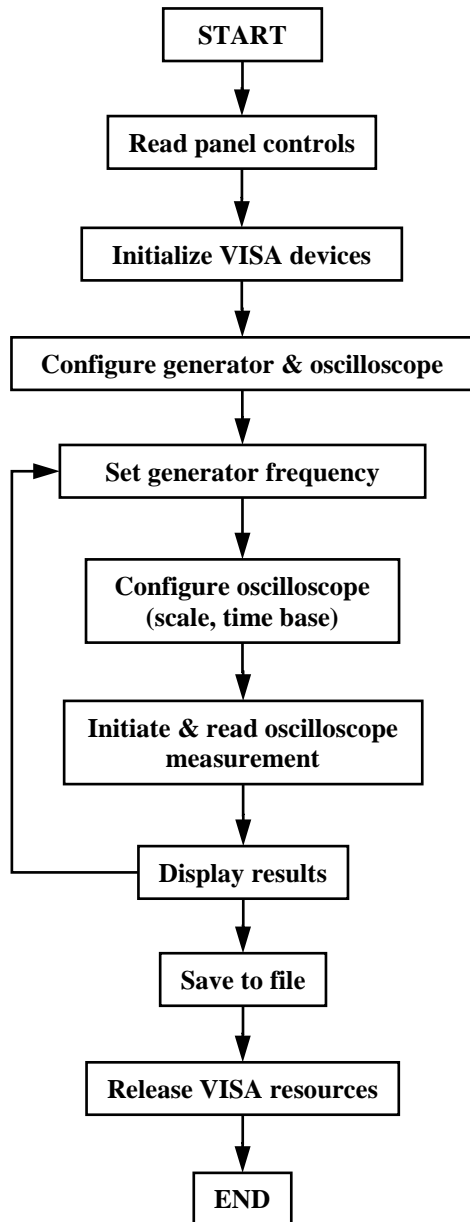


Fig. 2. Simplified algorithm of the control software

II. PASS CHARACTERISTICS MEASUREMENT

Exemplary measurements have been performed for two types of 230V AC/50 Hz power-line cables. Cable no. 1 is a single insulation 2x1 mm², 50 m length without connectors. Cable no. 2 is a double insulation 3x2.5 mm², 100 m length with connectors. Both cables are stranded wires.

The measurement frequencies were divided into two ranges: low (10 kHz – 1 MHz) and high (1 MHz – 10 MHz). The low band is related to the European CENELEC A–D bands (covering 30 – 148.5 kHz), Japanese ARIB (155 – 403 kHz) and FCC (155 – 487 kHz) for the US and the rest of the world [15]. These bands are often used for automatic meter reading (AMR) and home control applications.

First measured parameter was pass characteristics. The amplitude characteristics represents voltage gain (inverse of insertion loss) and phase characteristics depends i.a. on cable length. The transmitter has been additionally equipped with high frequency separating transformer (model 744834405, Würth Elektronik) [16]. This eliminated problems of hardware equipment common grounding. Generator (transmitter) with transformer and oscilloscope (receiver) are connected by the measured cable (line under test, fig. 3).

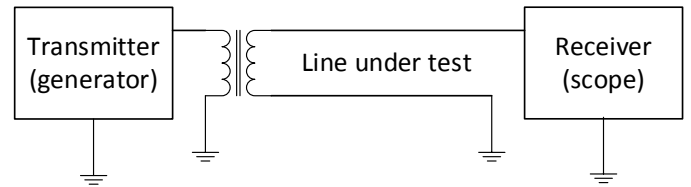


Fig. 3. Schematic for pass characteristics measurement

Output impedance of the generator was constant and equal 50 Ω. Input impedance of the oscilloscope was set to 1 MΩ || 11.5 pF. Fig. 4, 5 present amplitude characteristics and fig. 6, 7 phase characteristics. Term *trafo* denotes characteristics of the transformer itself, in order to compare its parameters with line parameters. Voltage gain of the transformer itself is reduced by 10 on the fig. 6 (*trafo x 0.1*) in order not to dominate other characteristics.

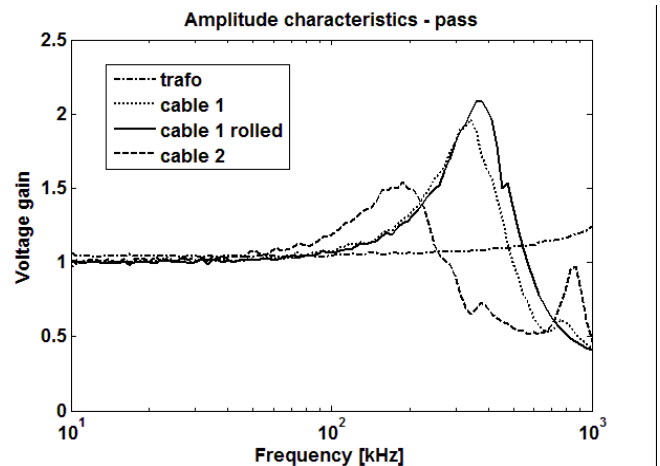


Fig. 4. Voltage gain for low band

The first cable has been measured in two scenarios: straight and rolled (ca. 25 cm diameter, 65 turns). The second cable has always been straightened. Both cables were placed in a building (concrete) environment.

The transformer influence is minimal below 2 MHz, while line influence (for particular lengths) can be neglected below 50 kHz. Above this value there can be observed +100%/-50% variation of the voltage gain.

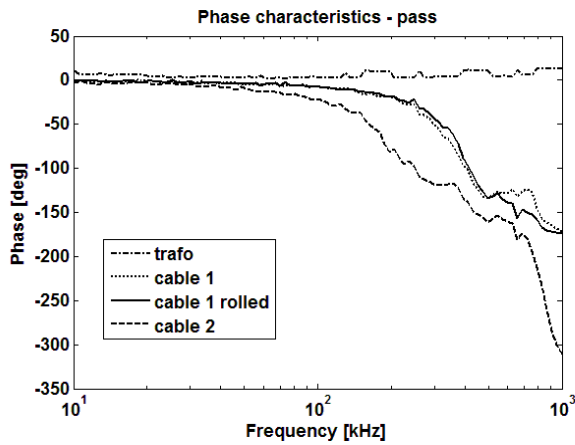


Fig. 5. Phase characteristics for low band – pass case

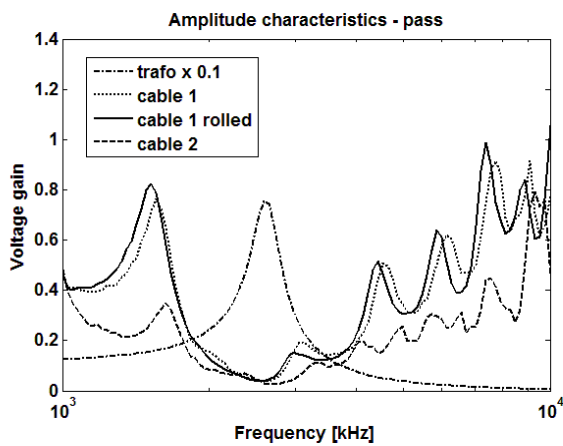


Fig. 6. Voltage gain for high band.

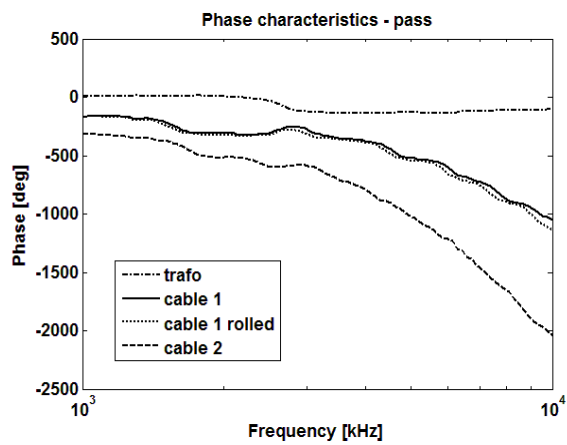


Fig. 7. Phase characteristics for high band – pass case

TABLE I
PASS CHARACTERISTICS – VOLTAGE GAIN

Band [MHz]	Minimal gain		Maximal gain	
	[V/V]	[dB]	[V/V]	[dB]
0.01 – 1	0.4	-8	2.1	6.4
1 – 10	0.04	-28	1.05	0.4

Pass amplitude characteristics becomes more complex in high band. Voltage gain drops below 1 with a minimum between 2 and 3 MHz, where strong resonance with the separating transformer occurs. Table 1 summarises extreme values of

voltage gain for pass characteristics. Generally, measured voltage gain was in a range $-28 \div +6$ dB, which calculates for total dynamics of 34 dB. This still represents smaller attenuation and smaller dynamics than e.g. for wireless links [17]. Total measurement time took 1.5 min. (for 100 points) and was dominated by the oscilloscope processing time.

III. CROSSTALK MEASUREMENT

Another important phenomena in PLC transmission is crosstalk between neighbourhood lines. Expected levels are high, because of lack of twisting and screening between particular lines/cables. The crosstalk measurements were performed for four scenarios:

1. at the end of passive line, with active line open (fig. 8, fig. 12 solid line, fig. 13 dashed line),
2. at the end of passive line, with active line short (fig. 9, fig. 12 dotted line, fig. 13 dash-dotted line),
3. at the beginning of passive line, with active line open (fig. 10, fig. 12 dash-dotted line, fig. 13 dotted line),
4. at the beginning of passive line, with active line short (fig. 11, fig. 12 dashed line, fig. 13 solid line).

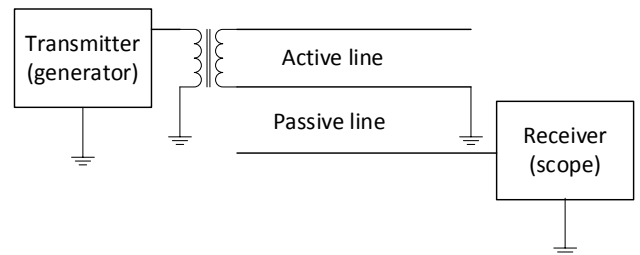


Fig. 8. Cross-talk measurement – scenario 1

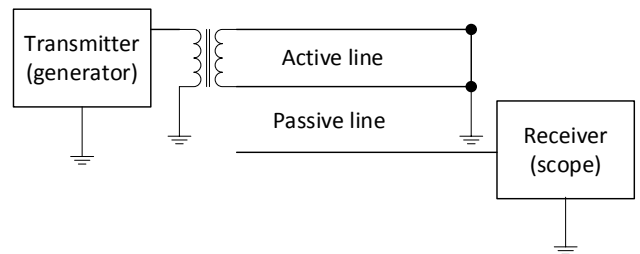


Fig. 9. Cross-talk measurement – scenario 2

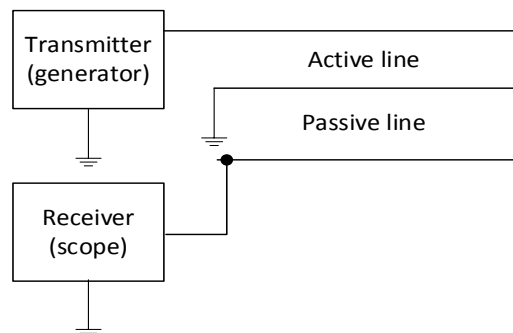


Fig. 10. Cross-talk measurement – scenario 3

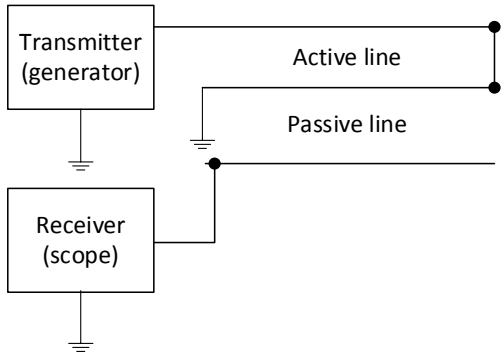


Fig. 11. Cross-talk measurement – scenario 4

The last two measurements (scenarios 3 and 4) were taken without coupling transformer. The term *active line* denotes a cable where generator was connected (*signal injection*) and the term *passive line* denotes a cable where oscilloscope was connected (signal reception). The third cable was common and grounded.

As expected, there can be observed high coupling between lines. The most common case (distant receiver with high impedance load) presents voltage coupling in range 0.06 – 0.7 (-24 ÷ -3.1 dB), mainly for lower band. Dynamics range of crosstalk for this case is the highest: nearly 20 dB. There can be also observed a wide spectrum (2 – 4 MHz) of relatively low crosstalk level. Table 2 summarises its extreme values.

IV. SPLIT PATH EXAMPLES

Another measurements considered two scenarios of split transmission path. Two 50 m sections of cable no. 2 were connected with additional *split*: at the end (fig. 14) or at the beginning (fig. 15). The cables have been open (unloaded) at the ends in both cases.

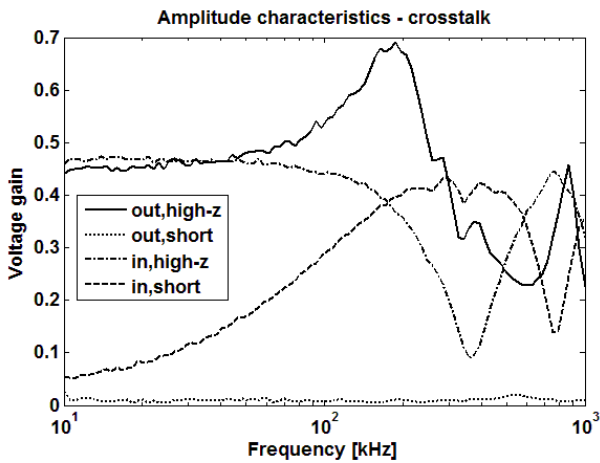


Fig. 12. Cross-talk measurement for low band – amplitude characteristics

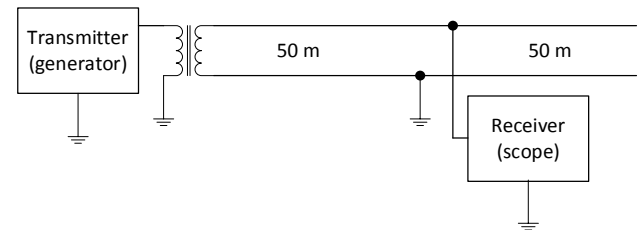


Fig. 14. Split path measurement schematic – split at the end

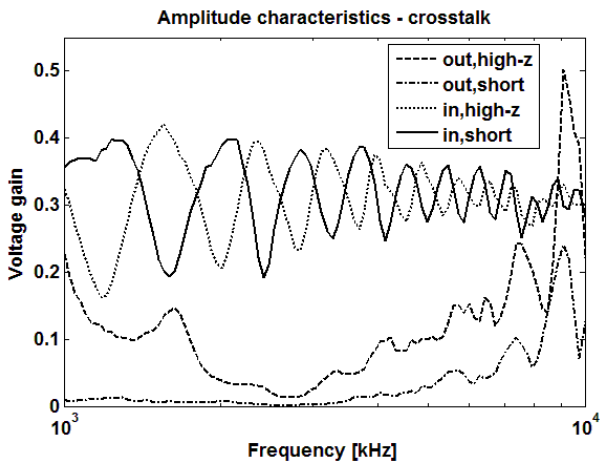


Fig. 13. Cross-talk measurement for high band – amplitude characteristics

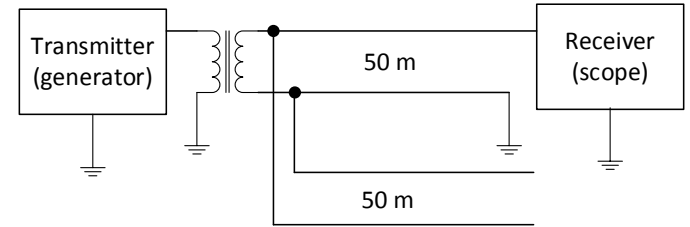


Fig. 15. Split path measurement schematic – split at the beginning

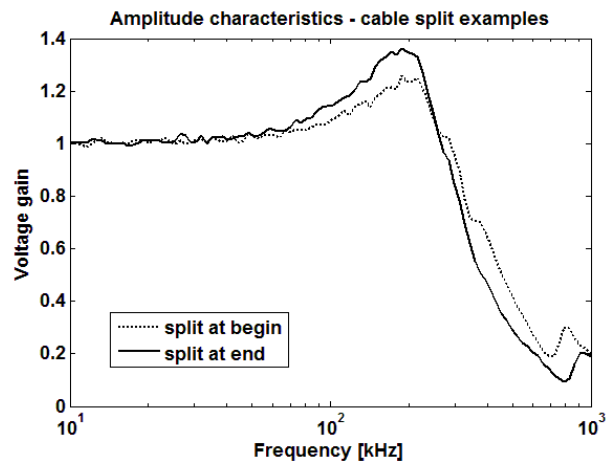


Fig. 16. Split path measurement – low band

TABLE II
CROSSTALK CHARACTERISTICS

Band [MHz]	Minimal		Maximal	
	[V/V]	[dB]	[V/V]	[dB]
0.01 – 1	0.03	-30	0.7	-3.1
1 – 10	0.02	-34	0.5	-6

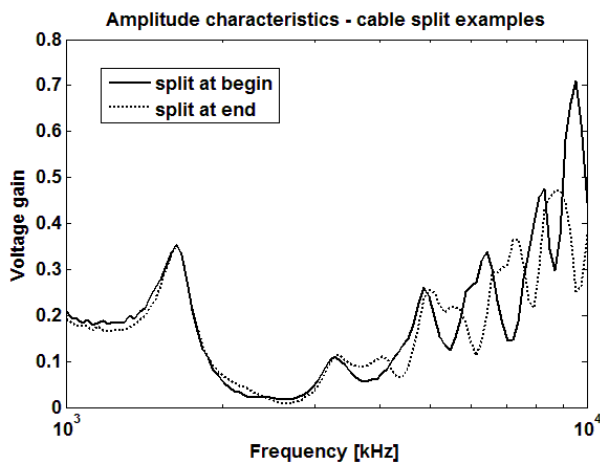


Fig. 17. Split path measurement – high band

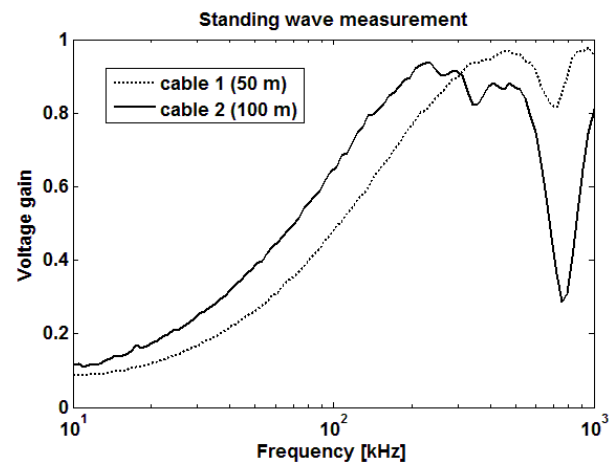


Fig. 19. Standing waves in low band

TABLE III
SPLIT EXAMPLE

Band [MHz]	Minimal		Maximal	
	[V/V]	[dB]	[V/V]	[dB]
0.01 – 1	0.1	-20	1.38	2.8
1 – 10	0.02	-34	0.71	-3

Comparing to the single line connection, influence of split is visible, however line behaviour remains similar (fig. 16, 17). Dynamics increases to 37 dB. Table 3 summarises extreme values of voltage gain for split cables.

V. OTHER LINE PARAMETERS

Based on standing wave measurement, velocity factor of the cable can be calculated. Measurement at the input of short line has been performed according to fig. 18. Both cables were investigated. In case of cable no. 2, unused third wire has been left unconnected. Fig. 19 and 20 present normalised voltage on input of the lines.

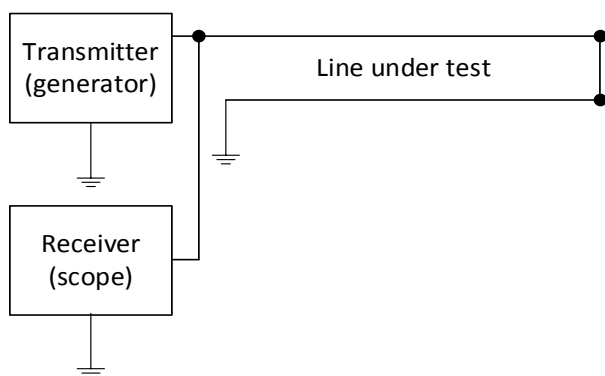


Fig. 18. Standing waves measurement

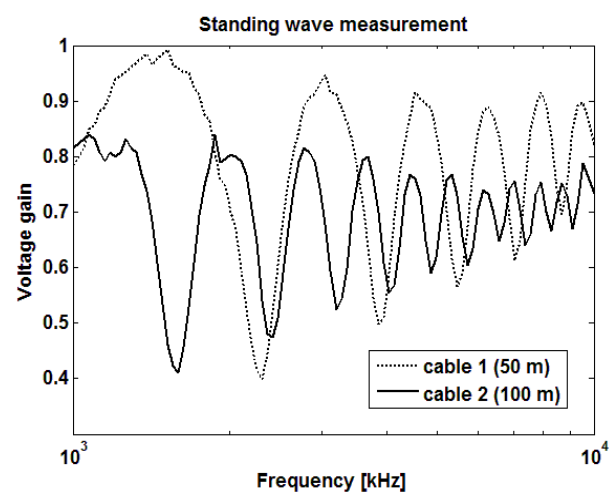


Fig. 20. Standing waves in high band

TABLE IV
STANDING WAVE EXTREMA (CABLE NO. 1, 50 M)

	Freq. [MHz]	Air wavelength [m]	Cable wavelength [m]	Velocity factor
1 st min	2.31	130	100	0.78
2 nd min	3.85	78	50	0.64
3 rd min	5.46	55	33	0.66
1 st max	1.4*	214*	200*	0.9*
2 nd max	3	100	67	0.67
3 rd max	4.7	64	40	0.63

TABLE V
STANDING WAVE EXTREMA (CABLE NO. 2, 100 M)

	Freq. [MHz]	Air wavelength [m]	Cable wavelength [m]	Velocity factor
1 st min	0.75	400	200	0.5
2 nd min	1.62	187	100	0.53
3 rd min	2.42	124	67	0.54
1 st max	0.3*	1000*	400*	0.4*
2 nd max	1.5*	200*	133	0.66*
3 rd max	2	150	80	0.53

Estimation of selected coordinates of the maxima and minima from fig. 19, 20 are presented in tables 4, 5 respectively. Based on these values it can be assumed that velocity factor for cable no. 1 equals ca 0.6 – 0.7 and for cable no. 2 ca 0.5 – 0.6. Note that some readouts contain large uncertainty, even for large (“clean”) values of measured signal. They have been marked with asterisks. The result is calculation of the velocity factor with the smallest accuracy – tab. 4, 5.

VI. TIME-DOMAIN EXAMPLES

The last example has been performed in time-domain for unipolar (0 – 3 V) rectangular signal with 100 kHz frequency. Such signal can mimic e.g. digital transmission at rate 200 kbps. There have been used measurement setup from fig. 3 and 100 m of cable no. 2. Fig. 21 presents received (distorted) signal for $1\text{ M}\Omega \parallel 11.5\text{ pF}$ load impedance. Despite of visible influence of reflections and narrow band of coupling transformer, the received signal can be recognised and decoded correctly, however positive and negative overshoots exceeding 1 V require attention (e.g. protection circuitry). Fig. 22 presents abovementioned case for $50\ \Omega$ load impedance – lower waveform is the received signal. Although these figures were observed directly on the scope, it is easy and fast to include such functionality in the virtual instrument. This would be helpful for estimation of time-domain behaviour and/or complex-spectrum signals.

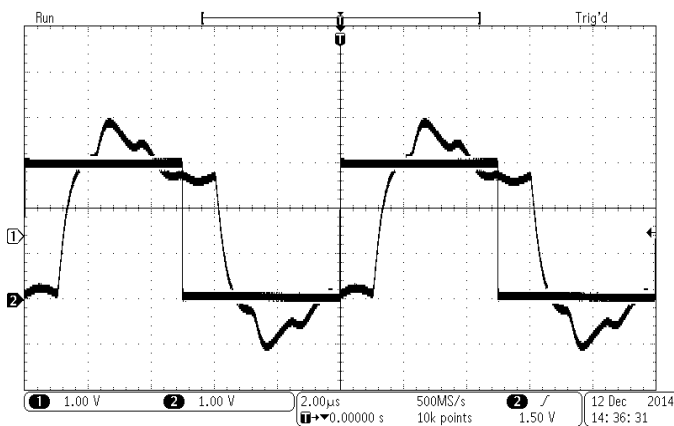


Fig. 21. Digital signal in time-domain, $R_{\text{load}} = 1\text{ M}\Omega$

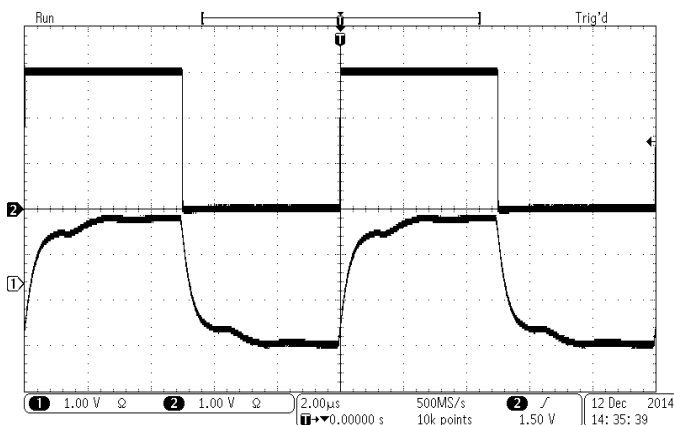


Fig. 22. Digital signal in time-domain, $R_{\text{load}} = 50\ \Omega$

VII. SUMMARY

Power-line communication techniques are known and practically used since 20's of the XX century. Despite of undisputable advantages (wide availability of transmission medium, relatively low signal attenuation, low modems cost) they did not become massively used. Unpredictable and still non-

standardised power lines and devices for high frequency operation are challenge for PLC designers and users. The greatest problem is very low impedance of a supply AC source (as visible form a socket terminals). This behaviour is designed and expected, because grid parameters must be well stabilised. However, it effectively shorts any signals generated at socket terminals. Even, if this problem is solved e.g. by using mains with separating phase inductances (high impedance for PLC bands), other problems may occur. Common examples are: shunt capacitors (low parallel impedance), built-in coils (high series impedance), unpredictable phase connections, variable number of connected loads and variable grid impedance. A practical case is "a silent surprise", when no PLC communication occurs in possibly good transmission conditions. This case has been result of a series inductance found in a local fuse. Therefore fast, automatic estimation of selected, high frequency line parameters facilitates design of PLC network.

LabVIEW environment simplifies creation of virtual device and allows easy extension of its functionality. The measurements in proposed system are not critical – both in terms of frequency range, levels and required accuracy. Therefore commonly available devices (generators, oscilloscopes) with appropriate buses (e.g. USB or Ethernet) and SCPI support are sufficient. The effect is practically useful and affordable automatic measurement stand.

REFERENCES

- [1] Dostert, K. In *Powerline Communications*; Prentice-Hall: New York USA, 2001.
- [2] Papadopoulos, A., Argyropoulos, G.C., Sarantinos, B.D., Papagiannis, G.K., *Analysis of Indoor PLC Networks: Laboratory Tests and Simulation Results*, IEEE Power Tech, Lausanne, pp. 1935,1940, 1-5 July 2007.
- [3] Papadopoulos, T.A., Papagiannis, G.K., Dokopoulos, P.S., *Low-Voltage Distribution Line Performance Evaluation for PLC Signal Transmission*, Power Delivery, IEEE Transactions on, vol. 23, no. 4, pp. 1903, 1910, Oct. 2008.
- [4] Razazian, K., Yazdani, J., *CENELEC and powerline communication specification in realization of smart grid technology*, Innovative Smart Grid Technologies (ISGT Europe), 2011 2nd IEEE PES International Conference and Exhibition on, pp.1,7, 5-7 Dec. 2011.
- [5] Buchner, P., Fender, M., *Compensation of low frequency harmonics caused by parallel operating AC converters*, Industrial Electronics, ISIE '96, Proceedings of the IEEE International Symposium on, vol. 2, pp. 618, 623, 17-20 Jun 1996.
- [6] Bmiller, G., *Evaluation and integrated diagnostic of high speed narrow band power-line chipset*, Power Line Communications and Its Applications, 2005 International Symposium on, pp. 371, 375, 6-8 April 2005.
- [7] Malack, J.A., Engstrom, J.R., *RF Impedance of United States and European Power Lines*, IEEE Trans. Electromag. Compat. 1976, 18, 36-38.
- [8] Guangbin Chu, Jianqi Li, Weilin Liu, *Narrow band power line channel characteristics for low voltage access network in China*, Power Line Communications and Its Applications (ISPLC), 17th IEEE International Symposium on, pp. 297, 302, 24-27 March 2013.
- [9] Gassara, H., Rouissi, F., Ghazel, A., *Statistical Characterization of the Indoor Low-Voltage Narrowband Power Line Communication Channel*, Electromagnetic Compatibility, IEEE Transactions on, vol. 56, no.1, pp. 123, 131, Feb. 2014.
- [10] Cooper, D. ; Jeans, T., "Narrow-Band, Low Data Rate Communications on the Low-Voltage Mains in the CENELEC Frequencies, Part 1: Noise

- and Attenuation”, *Power Engineering Review*, IEEE, vol. 22, iss. 4, pub. year 2002, Page(s): 75.
- [11] Bausch, J.; Kistner, T.; Moreau, A.; Sauvage, S.; Milanini, S., *Advanced "Orphelec" test equipment and novel test procedures*, *Power Line Communications and Its Applications*, 2005 International Symposium on, pp. 385, 389, 6-8 April 2005.
- [12] Sigle, M.; Bauer, M.; Wenqing Liu; Dostert, K., *Transmission channel properties of the low voltage grid for narrowband power line communication*, *Power Line Communications and Its Applications (ISPLC)*, 2011 IEEE International Symposium on, pp. 289, 294, 3-6 April 2011.
- [13] Maenou, T.; Katayama, M., *Study on Signal Attenuation Characteristics in Power Line Communications*, *Power Line Communications and Its Applications*, 2006, IEEE International Symposium on, pp. 217, 221.
- [14] Standard Commands for Programmable Instrumentation (SCPI) – IVI Foundation, <http://www.ivifoundation.org/scpi>
- [15] Berger, Lars T.; Schwager, Andreas; Schneider, Daniel M. “MIMO Power Line Communications: Narrow and Broadband Standards”, *EMC and Advanced Processing. Devices, Circuits, and Systems*, chapter 10. CRC Press. Feb. 2014, ISBN 9781466557529.
- [16] <http://katalog.we-online.de/pbs/datasheet/744834405.pdf>
- [17] I. Hakki Cavdar, Engin Karadeniz, *Measurements of Impedance and Attenuation at CENELEC Bands for Power Line Communications Systems*, *Sensors* 2008, vol. 8, pp. 8027-8036, ISSN 1424-8220.